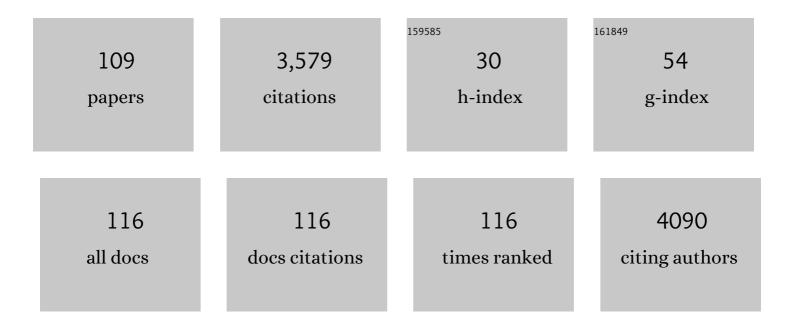
Justin M Notestein

List of Publications by Year in descending order

Source: https://exaly.com/author-pdf/8033655/publications.pdf Version: 2024-02-01



#	Article	IF	CITATIONS
1	Enhancing Heterogeneous Catalysis through Cooperative Hybrid Organic–Inorganic Interfaces. Chemistry - A European Journal, 2006, 12, 3954-3965.	3.3	231
2	Machine learning the quantum-chemical properties of metal–organic frameworks for accelerated materials discovery. Matter, 2021, 4, 1578-1597.	10.0	170
3	Tandem In ₂ O ₃ -Pt/Al ₂ O ₃ catalyst for coupling of propane dehydrogenation to selective H ₂ combustion. Science, 2021, 371, 1257-1260.	12.6	148
4	MOF-enabled confinement and related effects for chemical catalyst presentation and utilization. Chemical Society Reviews, 2022, 51, 1045-1097.	38.1	148
5	Periodic Trends in Highly Dispersed Groups IV and V Supported Metal Oxide Catalysts for Alkene Epoxidation with H ₂ 0 ₂ . ACS Catalysis, 2015, 5, 5077-5088.	11.2	115
6	Consequences of Confinement for Alkene Epoxidation with Hydrogen Peroxide on Highly Dispersed Group 4 and 5 Metal Oxide Catalysts. ACS Catalysis, 2018, 8, 2995-3010.	11.2	111
7	Shape-selective sieving layers on an oxide catalyst surface. Nature Chemistry, 2012, 4, 1030-1036.	13.6	110
8	Structure–Activity Relationships That Identify Metal–Organic Framework Catalysts for Methane Activation. ACS Catalysis, 2019, 9, 3576-3587.	11.2	105
9	Grafted Metallocalixarenes as Single-Site Surface Organometallic Catalysts. Journal of the American Chemical Society, 2004, 126, 16478-16486.	13.7	95
10	Identifying promising metal–organic frameworks for heterogeneous catalysis via highâ€ŧhroughput periodic density functional theory. Journal of Computational Chemistry, 2019, 40, 1305-1318.	3.3	87
11	Stable Metal–Organic Framework-Supported Niobium Catalysts. Inorganic Chemistry, 2016, 55, 11954-11961.	4.0	85
12	Synthesisâ^'Structure–Function Relationships of Silica-Supported Niobium(V) Catalysts for Alkene Epoxidation with H ₂ 0 ₂ . ACS Catalysis, 2016, 6, 6124-6134.	11.2	78
13	The First Single-Step Immobilization of a Calix-[4]-arene onto the Surface of Silica. Chemistry of Materials, 2002, 14, 3364-3368.	6.7	76
14	Pushing the Limits on Metal–Organic Frameworks as a Catalyst Support: NU-1000 Supported Tungsten Catalysts for <i>o</i> -Xylene Isomerization and Disproportionation. Journal of the American Chemical Society, 2018, 140, 8535-8543.	13.7	73
15	Tuning the Redox Activity of Metal–Organic Frameworks for Enhanced, Selective O ₂ Binding: Design Rules and Ambient Temperature O ₂ Chemisorption in a Cobalt–Triazolate Framework. Journal of the American Chemical Society, 2020, 142, 4317-4328.	13.7	67
16	Photoluminescence and Charge-Transfer Complexes of Calixarenes Grafted on TiO2 Nanoparticles. Chemistry of Materials, 2007, 19, 4998-5005.	6.7	65
17	Structural Assessment and Catalytic Consequences of the Oxygen Coordination Environment in Grafted Tiâ ^{°2} Calixarenes. Journal of the American Chemical Society, 2007, 129, 1122-1131.	13.7	65
18	The Role of Outer-Sphere Surface Acidity in Alkene Epoxidation Catalyzed by Calixareneâ^'Ti(IV) Complexes. Journal of the American Chemical Society, 2007, 129, 15585-15595.	13.7	61

#	Article	IF	CITATIONS
19	Computational Predictions and Experimental Validation of Alkane Oxidative Dehydrogenation by Fe ₂ M MOF Nodes. ACS Catalysis, 2020, 10, 1460-1469.	11.2	53
20	The Role of Amine Surface Density in Carbon Dioxide Adsorption on Functionalized Mixed Oxide Surfaces. ChemSusChem, 2011, 4, 1671-1678.	6.8	51
21	Depositing SiO ₂ on Al ₂ O ₃ : a Route to Tunable BrÃ,nsted Acid Catalysts. ACS Catalysis, 2016, 6, 6156-6164.	11.2	50
22	Adsorption of <i>n</i> -Butanol from Dilute Aqueous Solution with Grafted Calixarenes. Langmuir, 2011, 27, 11990-11998.	3.5	46
23	Grafted Ta–calixarenes: Tunable, selective catalysts for direct olefin epoxidation with aqueous hydrogen peroxide. Journal of Catalysis, 2010, 275, 191-201.	6.2	44
24	Manganese Triazacyclononane Oxidation Catalysts Grafted under Reaction Conditions on Solid Cocatalytic Supports. Journal of the American Chemical Society, 2011, 133, 18684-18695.	13.7	44
25	High-throughput predictions of metal–organic framework electronic properties: theoretical challenges, graph neural networks, and data exploration. Npj Computational Materials, 2022, 8, .	8.7	43
26	Silica support modifications to enhance Pd-catalyzed deoxygenation of stearic acid. Applied Catalysis B: Environmental, 2016, 192, 93-100.	20.2	40
27	Well-Defined Diblock Copolymers via Termination of Living ROMP with Anionically Polymerized Macromolecular Aldehydes. Macromolecules, 2002, 35, 1985-1987.	4.8	36
28	Understanding the Hydrodenitrogenation of Heteroaromatics on a Molecular Level. ACS Catalysis, 2016, 6, 1455-1476.	11.2	34
29	Energetics of Small Molecule and Water Complexation in Hydrophobic Calixarene Cavities. Langmuir, 2006, 22, 4004-4014.	3.5	32
30	Role of surface reconstruction on Cu/TiO2 nanotubes for CO2 conversion. Applied Catalysis B: Environmental, 2019, 255, 117754.	20.2	32
31	The Synthesis Science of Targeted Vapor-Phase Metal–Organic Framework Postmodification. Journal of the American Chemical Society, 2020, 142, 242-250.	13.7	32
32	Surface speciation and alkane oxidation with highly dispersed Fe(III) sites on silica. Journal of Catalysis, 2011, 279, 103-110.	6.2	31
33	Size-Selective Synthesis and Stabilization of Small Silver Nanoparticles on TiO ₂ Partially Masked by SiO ₂ . Chemistry of Materials, 2015, 27, 1269-1277.	6.7	31
34	Rate and Selectivity Control in Thioether and Alkene Oxidation with H ₂ O ₂ over Phosphonateâ€Modified Niobium(V)–Silica Catalysts. ChemCatChem, 2017, 9, 3714-3724.	3.7	31
35	Mechanism of Regioselective Ring-Opening Reactions of 1,2-Epoxyoctane Catalyzed by Tris(pentafluorophenyl)borane: A Combined Experimental, Density Functional Theory, and Microkinetic Study. ACS Catalysis, 2018, 8, 11119-11133.	11.2	31
36	The effect of support morphology on CoOX/CeO2 catalysts for the reduction of NO by CO. Journal of Catalysis, 2018, 366, 150-158.	6.2	31

#	Article	IF	CITATIONS
37	Quantifying accessible sites and reactivity on titania–silica (photo)catalysts: Refining TOF calculations. Journal of Catalysis, 2014, 309, 156-165.	6.2	30
38	Cyclohexane oxidative dehydrogenation over copper oxide catalysts. Journal of Catalysis, 2016, 341, 180-190.	6.2	30
39	A heterogeneous, selective oxidation catalyst based on Mn triazacyclononane grafted under reaction conditions. Chemical Communications, 2010, 46, 1640.	4.1	28
40	Realizing the data-driven, computational discovery of metal-organic framework catalysts. Current Opinion in Chemical Engineering, 2022, 35, 100760.	7.8	28
41	<i>In Situ</i> Characterization of Highly Dispersed, Ceria-Supported Fe Sites for NO Reduction by CO. Journal of Physical Chemistry C, 2015, 119, 4224-4234.	3.1	27
42	MOFs and their grafted analogues: regioselective epoxide ring-opening with Zr ₆ nodes. Catalysis Science and Technology, 2016, 6, 6480-6484.	4.1	27
43	Identifying Boron Active Sites for the Oxidative Dehydrogenation of Propane. ACS Catalysis, 2021, 11, 9370-9376.	11.2	27
44	Counting Active Sites on Titanium Oxide–Silica Catalysts for Hydrogen Peroxide Activation through Inâ€Situ Poisoning with Phenylphosphonic Acid. ChemCatChem, 2014, 6, 3215-3222.	3.7	26
45	Kinetic study of cyclooctene epoxidation with aqueous hydrogen peroxide over silica-supported calixarene–Ta(V). Applied Catalysis A: General, 2010, 387, 45-54.	4.3	25
46	Modulating Chemical Environments of Metal–Organic Framework-Supported Molybdenum(VI) Catalysts for Insights into the Structure–Activity Relationship in Cyclohexene Epoxidation. Journal of the American Chemical Society, 2022, 144, 3554-3563.	13.7	25
47	Role of Support Lewis Acid Strength in Copper-Oxide-Catalyzed Oxidative Dehydrogenation of Cyclohexane. ACS Catalysis, 2018, 8, 7598-7607.	11.2	24
48	Zr ₆ O ₈ Node-Catalyzed Butene Hydrogenation and Isomerization in the Metal–Organic Framework NU-1000. ACS Catalysis, 2020, 10, 14959-14970.	11.2	24
49	Supramolecular Porous Assemblies of Atomically Precise Catalytically Active Cerium-Based Clusters. Chemistry of Materials, 2020, 32, 8522-8529.	6.7	23
50	Catalyst structure and substituent effects on epoxidation of styrenics with immobilized Mn(tmtacn) complexes. Applied Catalysis A: General, 2016, 511, 78-86.	4.3	22
51	Multifunctional photo/thermal catalysts for the reduction of carbon dioxide. Catalysis Today, 2017, 280, 65-73.	4.4	22
52	Catalytic reduction of NO with H2 over redox-cycling Fe on CeO2. Applied Catalysis B: Environmental, 2015, 168-169, 68-76.	20.2	21
53	Fast Cyclohexane Oxidation Under Mild Reaction Conditions Through a Controlled Creation of Redoxâ€Active Fe(II/III) Sites in a Metalâ~'Organic Framework. ChemCatChem, 2019, 11, 5650-5656.	3.7	21
54	Heterometallic Ce ^{IV} /V ^V Oxo Clusters with Adjustable Catalytic Reactivities. Journal of the American Chemical Society, 2021, 143, 21056-21065.	13.7	21

#	Article	IF	CITATIONS
55	Strong electrostatic adsorption of Pt onto SiO2 partially overcoated Al2O3—Towards single atom catalysts. Journal of Chemical Physics, 2019, 151, 214703.	3.0	20
56	Structural and electronic promotion with alkali cations of silica-supported Fe(III) sites for alkane oxidation. Journal of Catalysis, 2012, 296, 77-85.	6.2	19
57	Predicting NO _{<i>x</i>} Catalysis by Quantifying Ce ³⁺ from Surface and Lattice Oxygen. ACS Applied Materials & Interfaces, 2017, 9, 30670-30678.	8.0	19
58	Enhancing the Regioselectivity of B(C ₆ F ₅) ₃ -Catalyzed Epoxide Alcoholysis Reactions Using Hydrogen-Bond Acceptors. ACS Catalysis, 2019, 9, 9663-9670.	11.2	19
59	Solid Cocatalysts for Activating Manganese Triazacyclononane Oxidation Catalysts. ACS Catalysis, 2011, 1, 1691-1701.	11.2	18
60	Synthesis and stabilization of small Pt nanoparticles on TiO2 partially masked by SiO2. Applied Catalysis A: General, 2018, 551, 122-128.	4.3	18
61	Comprehensive Phase Diagrams of MoS ₂ Edge Sites Using Dispersion-Corrected DFT Free Energy Calculations. Journal of Physical Chemistry C, 2018, 122, 15318-15329.	3.1	18
62	Isobutane Dehydrogenation over Bulk and Supported Molybdenum Sulfide Catalysts. Industrial & Engineering Chemistry Research, 2020, 59, 1113-1122.	3.7	18
63	Cyclohexene epoxidation with H ₂ O ₂ in the vapor and liquid phases over a vanadium-based metal–organic framework. Catalysis Science and Technology, 2020, 10, 4580-4585.	4.1	18
64	Vapor-phase ethanol carbonylation with heteropolyacid-supported Rh. Journal of Catalysis, 2015, 325, 1-8.	6.2	17
65	Vapor-Phase Cyclohexene Epoxidation by Single-Ion Fe(III) Sites in Metal–Organic Frameworks. Inorganic Chemistry, 2021, 60, 2457-2463.	4.0	17
66	Acceptorless Dehydrogenative Coupling of Neat Alcohols Using Group VI Sulfide Catalysts. ACS Sustainable Chemistry and Engineering, 2017, 5, 4890-4896.	6.7	16
67	Ni(ii) complex on a bispyridine-based porous organic polymer as a heterogeneous catalyst for ethylene oligomerization. Catalysis Science and Technology, 2017, 7, 4351-4354.	4.1	16
68	In-situ IR spectroscopy as a probe of oxidation/reduction of Ce in nanostructured CeO2. Applied Surface Science, 2018, 445, 548-554.	6.1	16
69	Comparing GGA, GGA+ <i>U</i> , and meta-GGA functionals for redox-dependent binding at open metal sites in metal–organic frameworks. Journal of Chemical Physics, 2020, 152, 224101.	3.0	16
70	Demonstrating the Critical Role of Solvation in Supported Ti and Nb Epoxidation Catalysts via Vapor-Phase Kinetics. ACS Catalysis, 2020, 10, 2817-2825.	11.2	16
71	Recovery of Dilute Aqueous Acetone, Butanol, and Ethanol with Immobilized Calixarene Cavities. ACS Applied Materials & Interfaces, 2014, 6, 289-297.	8.0	15
72	Strong Influence of the Nucleophile on the Rate and Selectivity of 1,2-Epoxyoctane Ring Opening Catalyzed by Tris(pentafluorophenyl)borane, B(C ₆ F ₅) ₃ . ACS Catalysis, 2019, 9, 11589-11602.	11.2	14

#	Article	IF	CITATIONS
73	Highâ€Valent Metal–Oxo Species at the Nodes of Metal–Triazolate Frameworks: The Effects of Ligand Exchange and Twoâ€State Reactivity for Câ"H Bond Activation. Angewandte Chemie - International Edition, 2020, 59, 19494-19502.	13.8	14
74	Increased productivity in ethylene carbonylation by zeolite-supported molybdenum carbonyls. Journal of Catalysis, 2016, 338, 313-320.	6.2	13
75	Identifying properties of low-loaded CoOX/CeO2 via X-ray absorption spectroscopy for NO reduction by CO. Journal of Catalysis, 2020, 381, 355-362.	6.2	13
76	Gas phase acceptorless dehydrogenative coupling of ethanol over bulk MoS2 and spectroscopic measurement of structural disorder. Journal of Catalysis, 2018, 366, 159-166.	6.2	12
77	Vapor phase ethanol carbonylation over Rh supported on zeolite 13X. Applied Catalysis A: General, 2016, 520, 122-131.	4.3	11
78	Evidence for Copper Dimers in Low-Loaded CuO _{<i>x</i>} /SiO ₂ Catalysts for Cyclohexane Oxidative Dehydrogenation. ACS Catalysis, 2018, 8, 9775-9789.	11.2	11
79	Catalytic dehydrogenation of isobutane over supported MoOx/K-Al2O3. Journal of Catalysis, 2021, 397, 212-222.	6.2	11
80	Microkinetic modeling of cis-cyclooctene oxidation on heterogeneous Mn–tmtacn complexes. Journal of Catalysis, 2012, 291, 17-25.	6.2	10
81	In situ FTIR spectroscopy of highly dispersed FeOx catalysts for NO reduction: Role of Na promoter. Catalysis Today, 2016, 267, 56-64.	4.4	10
82	Hybrid Approach for Selective Sulfoxidation via Bioelectrochemically Derived Hydrogen Peroxide over a Niobium(V)–Silica Catalyst. ACS Sustainable Chemistry and Engineering, 2018, 6, 7880-7889.	6.7	10
83	Direct Visualization of Independent Ta Centers Supported on Two-Dimensional TiO ₂ Nanosheets. Nano Letters, 2019, 19, 8103-8108.	9.1	10
84	Controlled Deposition of Silica on Titania-Silica to Alter the Active Site Surroundings on Epoxidation Catalysts. ACS Catalysis, 2020, 10, 13008-13018.	11.2	10
85	Graftable chiral ligands for surface organometallic materials: calixarenes bearing asymmetric centers directly attached to the lower rim. New Journal of Chemistry, 2008, 32, 1314.	2.8	9
86	Increasing the Aromatic Selectivity of Quinoline Hydrogenolysis Using Pd/MOx–Al2O3. Catalysis Letters, 2014, 144, 1832-1838.	2.6	9
87	The role of iodide promoters and the mechanism of ethylene carbonylation catalyzed by molybdenum hexacarbonyl. Journal of Catalysis, 2014, 319, 211-219.	6.2	9
88	Highâ€Valent Metal–Oxo Species at the Nodes of Metal–Triazolate Frameworks: The Effects of Ligand Exchange and Two‧tate Reactivity for Câ"H Bond Activation. Angewandte Chemie, 2020, 132, 19662-19670.	2.0	9
89	Creating BrÃ,nsted acidity at the SiO2-Nb2O5 interface. Journal of Catalysis, 2021, 394, 387-396.	6.2	8
90	Synthesis of a family of peracid-silica materials and their use as alkene epoxidation reagents. Microporous and Mesoporous Materials, 2016, 225, 289-295.	4.4	6

#	Article	IF	CITATIONS
91	Exploring mechanistic routes for light alkane oxidation with an iron–triazolate metal–organic framework. Physical Chemistry Chemical Physics, 2022, 24, 8129-8141.	2.8	6
92	Mechanistic Investigation of Enhanced Catalytic Selectivity toward Alcohol Oxidation with Ce Oxysulfate Clusters. Journal of the American Chemical Society, 2022, 144, 12092-12101.	13.7	6
93	C–N bond hydrogenolysis of aniline and cyclohexylamine over TaOx–Al2O3. New Journal of Chemistry, 2016, 40, 6001-6004.	2.8	5
94	Investigating the effect of metal nuclearity on activity for ethylene hydrogenation by metal-organic-framework-supported oxy-Ni(II) catalysts. Journal of Catalysis, 2022, 407, 162-173.	6.2	5
95	Identifying Support Effects in Au-Catalyzed CO Oxidation. ACS Catalysis, 2021, 11, 11921-11928.	11.2	4
96	Improving and stabilizing fluorinated aryl borane catalysts for epoxide ring-opening. Applied Catalysis A: General, 2022, 636, 118601.	4.3	4
97	A tri-layer approach to controlling nanopore formation in oxide supports. Nano Research, 2019, 12, 1223-1228.	10.4	3
98	Covalent Grafting of <i>m</i> -Phenylene-Ethynylene Oligomers to Oxide Surfaces. Chemistry of Materials, 2010, 22, 5319-5327.	6.7	2
99	Photoâ€Initiated Reduction of CO 2 by H 2 on Silica Surface. ChemSusChem, 2018, 11, 1163-1168.	6.8	2
100	Submonolayer Is Enough: Switching Reaction Channels on Pt/SiO2 by Atomic Layer Deposition. Journal of Physical Chemistry C, 2021, 125, 18725-18733.	3.1	2
101	Assessment of catalysts for oxidative coupling of methane and ethylene. Catalysis Today, 2023, 416, 113770.	4.4	2
102	Interfacial Unit-Dependent Catalytic Activity for CO Oxidation over Cerium Oxysulfate Cluster Assemblies. ACS Applied Materials & Interfaces, 2022, 14, 33515-33524.	8.0	2
103	A Unique Qualitative GC Experiment for an Undergraduate Instrumental Methods Course Using Selective Photoionization Detectors. Journal of Chemical Education, 1998, 75, 360.	2.3	1
104	Promoter Effects on Catalyst Selectivity and Stability for Propylene Partial Oxidation to Acrolein. Catalysis Letters, 2020, 150, 826-836.	2.6	1
105	Molybdenum oxide and sulfide active sites for isobutane dehydrogenation with methanol as a probe molecule. Journal of Catalysis, 2022, 413, 498-508.	6.2	1
106	R. Åebesta (ed.): Enantioselective Homogeneous Supported Catalysis. Catalysis Letters, 2012, 142, 1150-1151.	2.6	0
107	Photo-Initiated Reduction of CO2 by H2 on Silica Surface. ChemSusChem, 2018, 11, 1135-1135.	6.8	0
108	Mapping the thermal entrenchment behavior of Pd nanoparticles on planar SiO2 supports. Nanoscale, 2020, 12, 14245-14258.	5.6	0

#	Article	IF	CITATIONS
109	Orientation of 1,1′-Bi-2-naphthol Grafted onto TiO ₂ . Journal of Physical Chemistry C, 2022, 126, 7980-7990.	3.1	0